Acta Geologica Polonica, Vol. 56 (2006), No. 4, pp. 463-484

The petrogenesis of late Precambrian felsic alkaline magmatism in south Sinai, Egypt

MOKHLES K. AZER

Geology Department, National Research Centre, Al-Behoos Str., 12622-Dokki, Cairo, Egypt.
E-mail: mokhles72@yahoo.com

ABSTRACT:

AZER, M.K. 2006. The petrogenesis of late Precambrian felsic alkaline magmatism in south Sinai, Egypt. *Acta Geologica Polonica*, **56** (4), 463-484. Warszawa.

Alkaline felsic magmatism represents the final phase of the late Precambrian acid magmatism in south Sinai. The studied felsic suites occur as dyke-like intrusions, exhibit features characteristic of A-type granites. There were two main cycles of magmatic activity separated by a period of magmatic quiescence, which led to a composition gap between them. The earlier cycle includes quartz syenite that represents the precursor of the A-type granite series in south Sinai, whereas the second cycle includes more felsic volcanic-subvolcanic intrusive complexes. Intrusion of the two cycles was controlled by the pre-existing structure and individual igneous bodies were emplaced in an extensional tectonic regime during a phase of fracturing and uplift at the end of the Pan-African orogeny. The high variability in geochemical signature of A-type magmas in south Sinai suggests a variety of petrologic processes and reservoirs which reflects the participation of an intraplate mantle reservoir and evolved continental crust. K-enrichment in the rhyolite is a primary feature and attributed to the effect of volatiles which accumulated in the upper part of the magma chamber. In general, A-type magmas in south Sinai can be differentiated according to their magma source and tectonic setting into (1) non-primitive A-type magma (A_{NP}) and (2) primitive A-type magma (A_P). The non-primitive A-type magma is commonly known in Sinai as Iqna granite, which belongs to the highly fractionated, late- to post-orogenic, calc-alkaline I-type granites. The primitive A-type magma shows within-plate geochemical characteristics and was emplaced in an anorogenic setting. It is distinguished further into: (i) a magma having characteristics indicative of OIB-mantle contribution (A_1), and (ii) magma derived from crustal sources (A_2).

Key words: Goza-Banat, El-Hajid, A-type magma, K-enrichment, Alkaline.

INTRODUCTION

The Precambrian complex is exposed over an area of 14000 km^2 in south Sinai. It constitutes, together with the basement rocks of the Eastern Desert of Egypt, the northwestern corner of the Arabo-Nubian Shield (ANS). The ANS is part of the East African orogen formed in the late Proterozoic (900–550 Ma) by accretion and amalgamation of oceanic and continental magmatic arcs during subduction and obduction of oceanic crust and closure of the Mozambique Ocean (KRÖNER 1985; KRÖNER & *al.* 1987; STERN 1994; LOIZENBAUER & *al.* 2001). Late stages of this orogenic cycle are marked by abundant intraplate magmatism, intraplate rifting, and transcurrent faulting

(BLASBAND & *al.* 2000; KUSKY & MATSAH 2003; JOHNSON 2003).

This paper concerns the felsic rocks of non-orogenic suites emplaced during the youngest igneous activity of late Precambrian age in south Sinai. The aim is to elucidate the nature of these rocks, their tectonic environment, their magma source, and modifying geological processes. The felsic rocks with A-type characteristics in south Sinai are additionally separated into several subgroups. New field and geochemical data are presented for the alkaline felsic suites of the Gebel Goza–Gebel Banat area and Gebel El-Hajid, and integrated with published data for A-type rocks in south Sinai to separate these rocks into subgroups.

GEOLOGICAL OUTLINE AND PREVIOUS WORK

South Sinai is largely occupied by granitic rocks intruded into metamorphic rocks which include metavolcanics and metasediments that are locally intruded by metaplutonic rocks. The metamorphic rocks are preserved in four large regions, including the Feiran-Solaf belt and the W. Kid, W. Sa'al and Taba areas; many smaller areas of metamorphic rocks are scattered throughout the Sinai massif. The granites were compositionally divided into older grey granites of tonalite to granodiorite composition and younger pink and red granites of granite composition (EL-RAMLY & AKAAD 1960). EL-GABY (1975) proposed that these granites constitute one continuous series, and that the alkaline to peralkaline granites constitute a side-branch of minor subvolcanic intrusions. Later, EL-GABY & AHMED (1980) noted that the highly fractionated calc-alkaline, two-feldspar granite of Gebel Ma'in is intruded by the less fractionated quartz syenite of Gebel Goza, and accordingly considered the latter as independent magma constituting an alkaline to peralkaline granite series. This series is equivalent to G_3-granite of HUSSEIN & *al.* (1982) which is equated with the anorogenic A-type granites. G_3-granite comprises a vast array of leucocratic granites and syenites that are widly distributed in time and space; they range in age from late Precambrian to late Mesozoic.

The alkaline felsic rocks of G[1]. Goza–G. Banat, and G. El-Hajid in central South Sinai (Text-fig. 1A) occur as elongate dyke-like bodies. They belong to the youngest igneous activity of late Precambrian age in south Sinai which formed a great number of small hypabyssal igneous intrusions. They are commonly associated with or intruded into subaerial, alkaline to peralkaline volcanics of comparable chemical composition (BENTOR & EYAL 1987), for which the name Katherina Volcanics of the Katherina Superprovince has been proposed (AGRON & BENTOR 1981). The Katherina Superprovince is formed essentially of alkaline volcanic and subvolcanic rocks comprising alkali granites and alkali rhyolites (including comendites and pantellerites).

Quartz syenite of G. Goza–G. Banat

Quartz syenites are limited in abundance and distribution in south Sinai compared to the other granitoids. The quartz syenite is intruded into the Feiran-Solaf gneiss belt and both older and younger calc-alkaline granitoids (Text-fig. 1B). Chilled margins occur along its contacts with the granites. The country rocks are intruded by various dykes that abut against the quartz syenites. The Feiran-Solaf gneiss belt includes gneisses and migmatites, together with subordinate schists, para- and ortho- amphibolites, and calc-silicates (EL-GABY & AHMED 1980; EL-TOKHI 1990; EL-SHAFEI & KUSKY 2003). The older and younger granites are calc-alkaline and subduction-related (EL-SHESHTAWI 1984). The former includes quartz diorite and granodiorite, whereas the latter includes monzogranite and syenogranite. The migmatization age of the Feiran-Solaf gneiss belt is 643±41 Ma by the whole-rock Rb-Sr method (BIELSKI 1982). U-Pb zircon ages of some paragneisses of the Feiran-Solaf gneiss belt include an age of 632±3 Ma (STERN & MANTON 1987), while KRÖNER & *al.* (1990) reported a $^{207}Pb/^{206}Pb$ zircon age of 796±6 for diorite gneisses. The granodiorite that intruded into the Feiran-Solaf gneiss (EL-SHAFEI & KUSKY 2003) produced a U-Pb age of 787±7 Ma (STERN & MANTON 1987). The ages cited indicate that the intrusive granodiorite is older than the gneiss. The granodiorite age is questionable and may represent the age of zircon xenocrysts, since the granodiorite is intruded into the Feiran-Solaf gneiss belt.

The highest peak for the quartz syenite rises to 1510 m above sea level. The quartz syenite is pink

[1] The Arabic word for mountain is variously spelled, such as Jebel, Gebel or Jabal. In this contribution we use the "Gebel" (G.) for simplicity.

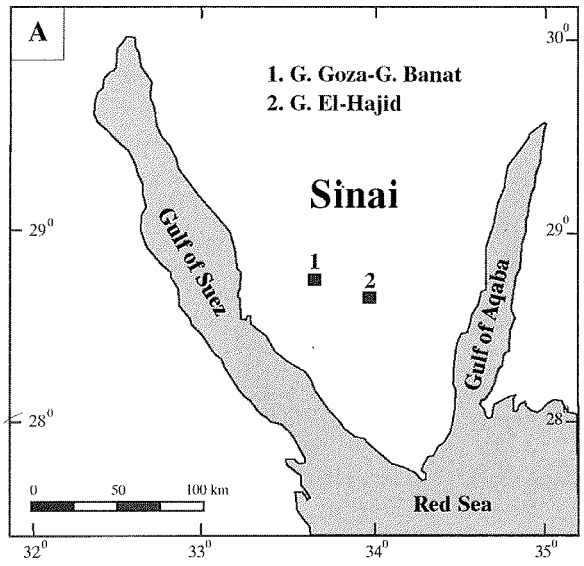

Fig. 1A. Location map of the felsic alkaline suites

in colour, homogeneous, and devoid of xenoliths. It was originally emplaced as an elongate dyke-like body along an ESE-WNW fault that was later dislocated by a fault trending NNE-SSW. On the Egyptian General Petroleum Corporation-CONOCO Oil Company (EGPC-CONOCO) geological map of Egypt (scale 1: 500 000, edited by KLITZSCH & *al.* 1987), the G. Goza–G. Banat quartz syenite is, however, grouped with the within-plate, alkaline Katherina Volcanics.

The volcanic-subvolcanic complex (VSC) of G. El-Hajid

The elongate intrusion of G. El-Hajid is composite in nature and consists of successive vertical sheets composed of alkali granite, porphyritic granite, and rhyolite. In the present work, the entire association is grouped as a volcanic-subvolcanic complex (VSC). It provides an excellent opportunity to study the A-type granites and their volcanic equivalents with the same tectonic setting and age. EYAL & HEZKIYAHU (1980) mapped the VSC of G. El-Hajid as an offshoot of the alkaline Katherina pluton. It is mapped on a recent geological map of Sinai issued by the Geological Survey of Egypt (sheet No. 1, scale 1 : 250 000; edited by EL-HINNAWI 1994) as a separate dyke-like intrusion related to the Katherina alkaline suite.

The VSC of G. El-Hajid occurs as a curved dyke-like body (Text-fig. 1C), about 18 km long and 0.3 to 1.25 km wide that was probably intruded along a pre-existing fracture related to cauldron subsidence. The peak of the intrusion rises to 1758 m above sea level. It is intruded with sharp contacts into calc-alkaline granites and alkali granites of late Precambrian age. The calc-alkaline granites belong geochemically and mineralogically to the subduction-related granitoids of an active continental margin tectonic setting (GHARIB & OBEID 2004)), while the alkali granites

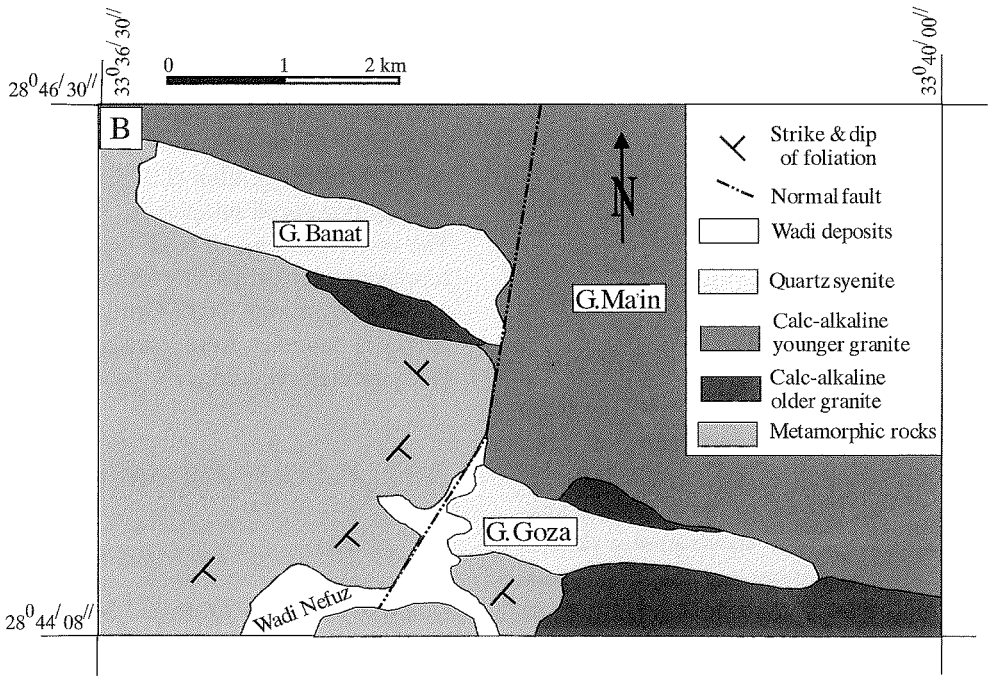

Fig. 1B. Geological map of G. Goza–G. Banat area (after EL-GABY & AHMED 1980)

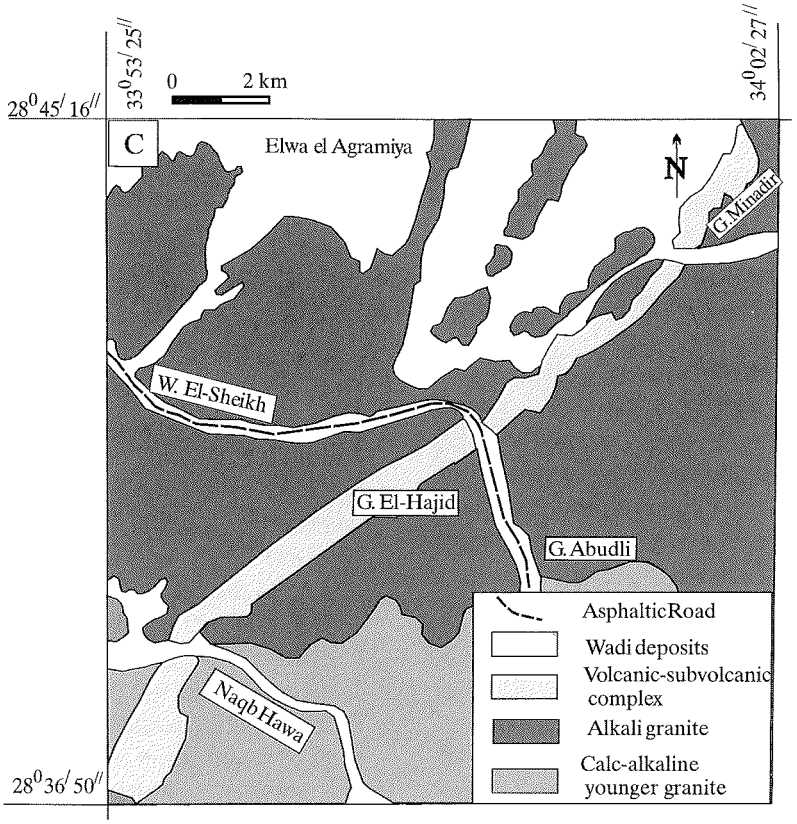

Fig. 1C. Geological map of the area around Gebel El-Hajid adopted from the geologic map of Sinai prepared by the Geological Survey of Egypt (Sheet No. 1, Scale 1: 250000, edited by EL-HINNAWI 1994)

exhibit within-plate, A-type characteristics (KATZIR & *al.* 2006). The alkali granite produced a Rb-Sr ages of 560±10 Ma (BIELSKI 1982) and 593±16 Ma (KATZIR & *al.* 2006). The granites of G. El-Hajid are massive, medium- to coarse-grained, and pink to red in colour both on fresh and weathered surfaces. The rhyolite is fine-grained and dissected by two well-developed joint systems. Dykes and exogenic xenoliths from the country rocks are absent.

ANALYTICAL TECHNIQUES

Polished thin sections of selected samples were examined with a Philips XL30 environmental scanning electron microscope (ESEM), operating at 25 kv and equipped with EDAX energy dispersive analytical X-ray sensitivity. The spectrometer detects elements with atomic number greater than 4 (e.g. B), with counting rate (per second) kept close to 1000-1500 counts. The ESEM analyses were carried out at the Nuclear Materials Authority in Egypt.

Twenty-six representative samples (12 quartz syenite, 9 alkali granite, 2 porphyritic granite, and 3 rhyolite) were analyzed for major and trace elements using X-ray fluorescence spectrometry (XRF) on fused-glass discs and pressed-powder pellets, respectively. The precision was generally better than ±5% for the major oxides and most trace elements. Loss on ignition (L.O.I.) was determined by heating powdered samples for one hour at 1000°C. The concentrations of REE were determined for 5 representative samples by inductively coupled plasma spectrometry (ICP-Optima 4300DV). The chemical analyses were carried out at the Saudi Geological Survey, Jeddah, Saudi Arabia.

PETROGRAPHY AND MINERALOGY

Petrography

Quartz syenite of G. Goza–G. Banat

The quartz syenite of G. Goza–G. Banat is medium-grained, inequigranular to porphyritic, and con-

sists of alkali feldspar, quartz, highly altered mafic minerals, and less common plagioclase. Alkali feldspar constitutes 65–85% of the rock and occurs as anhedral to euhedral crystals of orthoclase, orthoclase-perthite, and, less commonly, microcline. Most alkali feldspars are turbid and stained with pale, reddish-brown material. Quartz crystals (5–15% of the rock) occur as subhedral and as small anhedral, interstitial crystals. Plagioclase occurs as large phenocrysts and as small laths in the groundmass. Mafic minerals constitute 2.5–4.5% of the rock and include biotite and hornblende which are altered to chlorite and iron oxides. Biotite is represented by large tabular crystals and as fine interstitial flakes between other minerals. Hornblende occurs as anhedral to subhedral crystals enclosing Fe-Ti oxides and apatite inclusions. A few highly altered mafic xenocrysts, possibly pyroxene, are also present. The mafic xenocrysts have ovoid shape and/or irregular outlines that were later overgrown by an outer zone of K-feldspar. They are highly altered to chlorite and Fe-Ti oxides as well as secondary green amphibole. Xenocrysts show a spongy cellular texture due to the dissolution of these crystals by the enclosed magma under disequilibrium conditions. These xenocrysts may represent either a remnant high-temperature phase that crystallized at greater depths or possibly entrapped crystals. Accessories in the quartz syenite include Fe-Ti oxides, apatite, titanite and zircon; secondary minerals include epidote, chlorite, sericite and calcite.

The volcanic-subvolcanic complex of G. El-Hajid

The volcanic-subvolcanic complex of G. El-Hajid consists of three rock types, including alkali granite, porphyritic granite, and rhyolite.

The alkali granite is medium- to coarse-grained and hypidiomorphic inequigranular in texture. It consists mainly of perthite (60–70 vol.%), quartz (30–35 vol.%) and interstitial albite, with minor amounts of accessory fluorite, allanite, zircon, apatite, and Fe-Ti oxides. The prevalence of perthite in this rock indicates its hypersolvus nature. The perthites are represented by string, band, flame, and patch types. Quartz occurs as either large anhedral crystals or as graphic intergrowths with K-feldspar. Mafic minerals are represented mainly by clusters of biotite as well as alkali amphibole (Text-fig. 2A). Biotite occurs as subhedral flakes that are altered to chlorite, muscovite, epidote, and Fe-Ti oxides along cleavage planes and margins. Alkali amphibole is less common and occurs as fine anhedral crystals. Fluorite forms purple to colourless anhedral interstitial crystals (Text-fig. 2B). Allanite occurs as large, well-developed crystals with irregular terminations (Text-fig. 2C) or as fine dark brown grains. It alters to a dark brown metamict phase and is marginally replaced by muscovite and biotite. Miarolitic cavities filled by secondary quartz are observed locally.

The porphyritic granite is holocrystalline and fine- to medium-grained, spotted with phenocrysts. It consists mainly of K-feldspar and quartz, with minor biotite, albite, and fluorite. The granophyric texture is an outstanding feature (Text-fig. 2D); it is represented mainly by radial rims and spherulitic types. K-feldspar is the most common mineral and forms anhedral to subhedral crystals usually showing simple twinning. Rare K-feldspar phenocrysts are intergrown with quartz in a micrographic fashion. Quartz is present as individual crystals or intergrown with K-feldspar in the groundmass, developing granophyric and micrographic textures. Biotite occurs as small anhedral phenocrysts or as fine flakes in the groundmass that are altered to chlorite along the margins. Fluorite occurs as anhedral interstitial crystals or as veins along fractures traversing the rock (Text-fig. 2E) suggesting that fluorite is locally deuteric in origin (Tollo & *al.* 2004).

The rhyolite is fine-grained but speckled with variable amounts of phenocrysts (5–15% of the rock) which occur either as discrete crystals or as glomerophyric or cumulophyric aggregates. K-feldspar and quartz together with biotite and, less commonly, garnet, albite, and fluorite occur as phenocrysts set in a microcrystalline groundmass showing microgranular and micrographic textures. The K-feldspar phenocrysts are slightly altered and corroded by the groundmass. Quartz phenocrysts (<2 mm across) occur as subhedral to euhedral crystals showing square or hexagonal outlines and wavy extinction; globular phenocrysts of quartz are locally present. Garnet occurs as conspicuous euhedral to sub-rounded microphenocrysts (Text-fig. 2F) or as interstitial crystals in the groundmass. Fluorite occurs as microphenocrysts commonly associated with biotite or as fine crystals in the groundmass.

Mineralogy

The ESEM technique was used to identify some accessory minerals (garnet, fluorite and allanite) to

support the microscopic identification. Qualitative chemical analyses of these accessory minerals (normalized to 100%) are listed in Tables 1, 2 and 3.

Garnet phenocrysts occur only in the volcanic rocks of G. El-Hajid. They are euhedral to round in shape and devoid of inclusions and reaction rims, suggesting crystallization as a primary phase in equilibrium with the melt (ZEN 1988). JAHN & *al.* (2001, 2004) and WU & *al.* (2004) stated that garnets in A-type rocks could crystallize by a high degree of fractional crystallization coupled with intense fluid-magma interaction during the late stage of magmatic evolution. The garnet phenocrysts have the composition $Alm_{63.1\text{-}72.1}$ $Gross_{2.8\text{-}21.6}$ $Pyr_{1.8\text{-}13.3}$ $Spess_{8.3\text{-}25.4}$. The garnets are almandine-rich and the MnO content ranges from

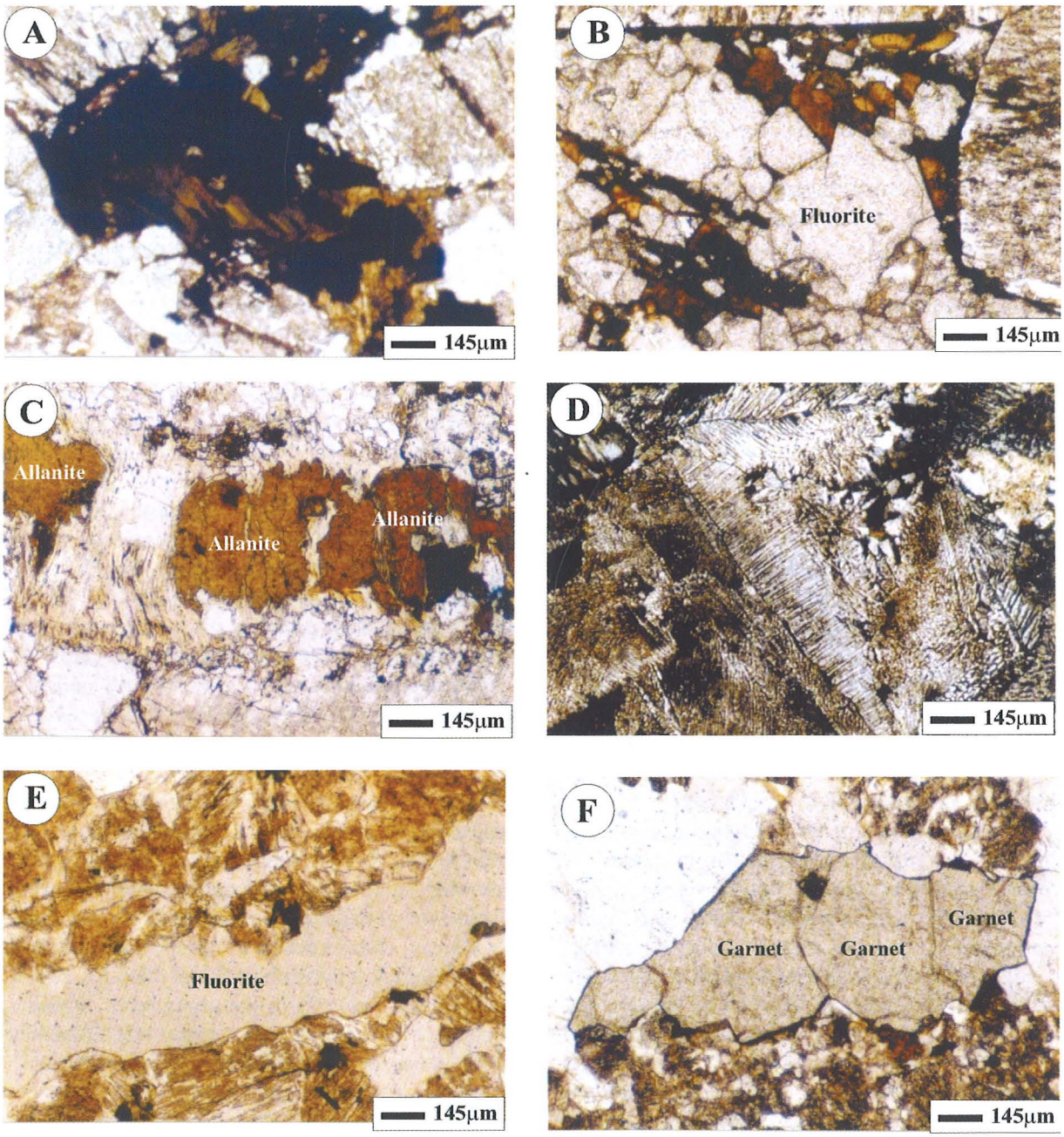

Fig. 2. (A) Clusters of biotite and alkali amphibole in the alkali granite; (B) Fluorite crystals in the alkali granite; (C) Allanite crystals replaced at periphery by muscovite in the alkali granite; (D) Granophyre texture in the porphyritic granite; (E) Fluorite vein in the porphyritic granite; (F) Garnet microphenocrysts in the rhyolite

Sample No.	V10			V30	
Spot No.	1	2	3	1	2
SiO_2	36.50	38.36	35.94	37.09	36.54
TiO_2	0.23	0.01	0.51	0.27	0.09
Al_2O_3	19.92	22.21	20.76	17.58	20.01
FeO	33.01	26.64	29.80	31.05	30.48
MnO	4.00	5.31	3.86	6.11	11.12
MgO	1.21	0.41	2.96	3.67	0.78
CaO	5.13	7.06	6.17	4.23	0.98
Total	100.00	100.00	100.00	100.00	100.00
Numbers of cations based on (12) oxygens					
Si	2.97	3.09	2.88	2.99	3.00
Al	1.91	2.10	1.96	1.67	1.94
Ti	0.01	0.00	0.03	0.02	0.01
Fe^{2+}	2.24	1.79	1.99	2.10	2.10
Mg	0.15	0.05	0.35	0.44	0.10
Mn	0.28	0.36	0.26	0.42	0.77
Ca	0.45	0.61	0.53	0.37	0.09
End members					
Almandine	72.09	63.74	63.56	63.11	68.67
Grossular	14.35	21.64	16.86	11.02	2.83
Pyrope	4.71	1.75	11.25	13.30	3.13
Spessartine	8.85	12.87	8.34	12.58	25.37

Tab. 1. Garnet from rhyolite

3.86 to 11.12% with an average 6.08% (Table 1), which indicates their crystallization at shallow depths (≤5 kbar, GREEN 1977).

Fluorite is observed in all rock types of G. El-Hajid as idiomorphic discrete crystals and locally as veins in the porphyritic granite. The individual fluorite crystals indicate its late crystallization from a magma at the end stage of crystallization. The thin fluorite veins, cutting through the porphyritic granite, most probably represent fluorine-rich hydrothermal solution emanating from the enclosing granite. The presence of fluorite indicates intense interaction of the residual melts with hydrothermal fluids rich in F (CHEN & JAHN 2004). CaF_2 constitutes 84.00 to 97.73 wt.% of the analyzed fluorite (Table 2); SiO_2, Al_2O_3 and K_2O occur in small amounts as impurities or inclusions.

Allanite, present in the alkali granite, contains considerable amounts of La_2O_3 (4.91 to 11.71 wt. %), Ce_2O_3 (9.89 to 19.87 wt.%) and Nd_2O_3 (3.62 to 15.35 wt.%) (Table 3). It is often metamict due to destruction of the crystalline structure by the bombardment of α-particles emitted by the radioactive constituents (DEER & *al.* 1992). Metamictization typically lowers the stability of allanite which, in turn, becomes more susceptible to alteration (see petrographic section).

GEOCHEMISTRY AND TECTONOMAGMATIC AFFINITY

Representative chemical analyses of the two felsic suites, as well as the calculated normative minerals, are given in Tables 4, 5, 6 and 7. Normative minerals are calculated using Minpet Software (RICHARD 1995). The quartz syenite of G. Goza–G. Banat shows limited compositional variation with SiO_2 ranging from 61.21 to 66.39 wt.%. It is characterized by relatively high abundance of total alkalis (9.79–11.73 wt.%), Al_2O_3 (15.18–16.90 wt.%), CaO (1.35–3.08 wt.%), Ba (716–1756 ppm), and Sr (116–281 ppm) relative to the VSC of G. El-Hajid.

Rock type	Rhyolite				Porphyritic granite			Alkali granite		
Sample No.	V10		V30		30A			300		
Spot No.	1	2	1	2	1	2	3	1	2	3
SiO_2	1.67	6.57	9.27	0.77	2.07	9.12	12.52	1.26	1.52	2.08
Al_2O_3	0.40	0.00	0.00	0.00	0.50	1.82	2.22	1.92	1.23	0.12
CaF_2	96.79	87.93	86.09	97.24	95.39	87.55	84.00	95.82	96.25	97.73
K_2O	0.05	0.48	0.38	0.36	0.48	1.05	0.83	0.77	0.50	0.07
Y_2O_3	1.09	5.02	4.26	1.63	1.56	0.46	0.43	0.23	0.50	0.00
Total	100.00	100.00	100.00	100.00	100.00	100.00	100.00	100.00	100.00	100.00

Tab. 2. Fluorite from rhyolite, porphyritic granite and alkali granite

Sample No.	300		100
Spot No.	1	2	1
SiO_2	21.75	32.73	29.61
Al_2O_3	15.21	11.06	13.95
FeO	8.63	7.01	14.28
CaO	14.28	9.96	16.94
La_2O_3	4.91	7.01	11.71
Ce_2O_3	19.87	18.31	9.89
Nd_2O_3	15.35	13.92	3.62
Total	100.00	100.00	100.00

Tab. 3. Allanite from alkali granite

Tab.4. Chemical compositions of the quartz syenite of G. Goza-G. Banat area

Sample	B1	B12	B15	B4	B6	G10	G11	G20	G6	G7	G8	G9
SiO_2	65.30	66.18	66.39	65.17	63.99	62.50	63.20	61.21	62.30	62.80	62.60	62.71
TiO_2	0.42	0.35	0.51	0.40	0.39	0.58	0.59	0.62	0.57	0.58	0.60	0.58
Al_2O_3	15.80	15.41	15.18	16.10	15.92	16.70	16.80	16.52	16.50	16.70	16.90	16.60
Fe_2O_3*	4.30	4.01	4.03	4.16	4.21	4.19	3.98	5.06	4.19	4.20	4.50	4.21
MnO	0.13	0.12	0.09	0.11	0.09	0.11	0.11	0.14	0.12	0.11	0.14	0.11
MgO	0.40	0.39	0.78	0.38	0.48	0.70	0.80	1.01	0.60	0.70	0.69	0.65
CaO	1.60	1.52	1.35	1.70	1.48	2.20	1.84	3.08	2.30	1.90	1.80	2.00
Na_2O	4.30	4.80	4.38	5.01	4.51	4.20	4.13	3.97	4.36	4.30	4.34	4.25
K_2O	5.96	6.31	6.12	6.72	6.14	6.21	6.50	5.82	6.32	6.21	6.24	6.11
P_2O_5	0.24	0.31	0.26	0.39	0.31	0.47	0.47	0.40	0.46	0.44	0.50	0.47
LOI	0.87	1.02	0.53	0.84	1.03	2.17	1.42	1.91	1.95	1.32	1.29	1.93
Total	99.32	100.42	99.62	100.98	98.55	100.03	99.84	99.74	99.67	99.26	99.6	99.62
Ba	716	1215	1041	1302	1342	1564	1517	1591	1586	1632	1756	1565
Rb	194	180	116	179	171	149	158	88	121	180	169	172
Sr	172	116	126	161	183	217	216	281	205	236	251	218
Y	29	29	32	35	30	26	27	29	25	24	28	27
Nb	19	21	23	24	25	16	16	14	15	18	19	17
Zr	465	416	366	491	392	309	270	257	272	224	297	255
Pb	93	30	56	95	25	270	141	116	176	163	142	210
V	0	13	8	9	8	11	12	30	11	11	13	11
Cr	4	11	0	5	18	3	0	0	5	4	2	0
Co	3	7	4	4	6	6	5	7	6	6	6	6
Ni	19	10	14	16	11	22	19	42	28	21	18	21
Cu	10	12	5	11	9	18	13	18	6	8	16	33
Zn	79	76	102	71	66	57	62	84	59	60	71	82
K_2O/Na_2O	1.39	1.31	1.40	1.34	1.36	1.48	1.57	1.47	1.45	1.44	1.44	1.44
K_2O+Na_2O	10.26	11.11	10.50	11.73	10.65	10.41	10.63	9.79	10.68	10.51	10.58	10.36
Y/Nb	1.53	1.38	1.39	1.46	1.20	1.63	1.69	2.07	1.67	1.33	1.47	1.59
Rb/Sr	1.13	1.55	0.92	1.11	0.93	0.69	0.73	0.31	0.59	0.76	0.67	0.79
K/Rb	255	291	438	312	298	346	342	549	434	286	307	295
Rb/Zr	0.42	0.43	0.32	0.36	0.44	0.48	0.59	0.34	0.44	0.80	0.57	0.67

* Total iron is expressed as Fe_2O_3

Tab. 5. Chemical compositions of the volcanic-subvolcanic complex of G. El-Hajid

Sample	Alkali granite									Porph. granite		Rhyolite		
	100	200	300	48	500	600	700	800	900A	30A	31	V10	V30	400
SiO_2	73.67	75.08	75.12	75.11	72.91	74.51	75.01	73.82	75.06	70.55	71.23	75.09	76.01	74.56
TiO_2	0.19	0.14	0.17	0.14	0.36	0.21	0.27	0.29	0.19	0.38	0.40	0.21	0.20	0.23
Al_2O_3	11.14	11.93	13.01	12.01	12.11	11.72	10.96	11.62	11.96	12.75	13.01	10.92	10.49	11.39
Fe_2O_3*	2.98	2.86	2.81	2.27	3.18	3.01	2.79	3.46	2.56	3.56	3.26	3.35	3.02	2.98
MnO	0.05	0.01	0.02	0.04	0.02	0.01	0.06	0.04	0.04	0.09	0.06	0.02	0.03	0.03
MgO	0.08	0.14	0.11	0.06	0.15	0.09	0.06	0.11	0.09	0.36	0.49	0.14	0.06	0.09
CaO	0.91	0.42	0.19	0.63	0.57	0.39	0.21	0.41	0.41	1.42	1.57	0.32	0.27	0.56
Na_2O	3.23	3.06	3.21	3.23	3.11	4.01	3.63	3.21	3.56	3.69	4.05	3.01	2.97	2.48
K_2O	4.71	4.99	4.92	5.11	5.01	5.16	5.26	4.97	4.86	5.11	4.92	6.08	6.11	6.49
P_2O_5	0.04	0.03	0.01	0.03	0.06	0.02	0.05	0.03	0.02	0.04	0.11	0.01	0.01	0.03
LOI	2.01	1.44	0.86	0.95	1.76	1.01	1.03	1.46	0.81	1.22	0.56	0.58	0.69	0.93
Total	99.01	100.1	100.43	99.58	99.24	100.14	99.33	99.42	99.56	99.17	99.66	99.73	99.86	99.77
Ba	192	212	101	37	314	142	236	128	64	417	456	102	49	121
Rb	257	201	196	206	210	238	198	187	212	163	172	186	179	239
Sr	41	25	16	65	51	32	28	47	15	85	61	23	19	21
Y	54	46	61	71	49	77	69	58	83	39	51	84	89	72
Nb	27	21	31	50	28	41	32	34	52	25	31	45	51	38
Zr	511	516	578	512	572	754	682	549	460	512	562	789	836	656
Pb	112	41	27	76	26	31	37	41	20	276	41	19	30	21
V	8	0	4	2	12	25	4	3	5	21	23	9	6	5
Cr	24	16	10	4	18	14	11	8	6	9	6	1	0	8
Co	2	0	0	2	1	2	3	1	0	0	1	1	2	1
Ni	63	102	96	10	76	138	98	76	10	14	15	5	10	56
Cu	41	91	20	7	8	12	23	10	6	6	16	1	36	26
Zn	54	41	67	146	38	21	83	96	86	211	101	93	118	31
K_2O/Na_2O	1.46	1.63	1.53	1.58	1.61	1.29	1.45	1.55	1.37	1.38	1.21	2.02	2.06	2.62
K_2O+Na_2O	7.94	8.05	8.13	8.34	8.12	9.17	8.89	8.18	8.42	8.80	8.97	9.09	9.08	8.97
Y/Nb	2.00	2.19	1.97	1.42	1.75	1.88	2.16	1.71	1.60	1.56	1.65	1.87	1.75	1.89
Rb/Sr	6.27	8.04	12.25	3.17	4.12	7.44	7.07	3.98	14.13	1.92	2.82	8.09	9.42	11.38
K/Rb	152	206	208	206	198	180	221	221	190	260	237	271	283	225
Rb/Zr	0.50	0.39	0.34	0.40	0.37	0.32	0.29	0.34	0.46	0.32	0.31	0.24	0.21	0.36

* Total iron is expressed as Fe_2O_3

Tab. 6. Normative mineral compositions for the quartz syenite of G. Goza–G. Banat area

	B1	B12	B15	B4	B6	G10	G11	G20	G6	G7	G8	G9
Quartz	13.3	11.48	13.93	7.5	10.51	9.16	9.88	9.17	7.89	9.46	15.05	9.96
Corundum	0	0	0	0	0	0.2	0.75	0	0	0.5	2.58	0.49
Orthoclase	35.23	37.3	36.17	39.72	36.29	36.7	38.42	34.4	37.35	36.7	36.88	36.11
Albite	36.38	40.61	37.9	42.39	38.16	35.54	34.94	33.59	36.89	36.38	28.26	35.96
Anorthite	6.21	0.51	0.35	1.6	5.07	7.84	6.06	6.77	6.79	6.55	5.66	6.85
Acmite	0	0	0	0	0	0	0	0	0	0	0	0
Diopside	0.13	4.22	3.81	3.59	0.21	0	0	4.85	1.34	0	0	0
Hypersthene	2.83	0.48	1.52	0.52	2.82	3.29	3.33	2.24	2.33	3.26	3.4	3.18
Magnetite	2.77	2.74	2.65	2.94	2.77	2.7	2.61	3.1	2.75	2.73	2.93	2.71
Ilmenite	0.8	0.59	0.97	0.76	0.74	1.1	1.12	1.37	1.08	1.1	1.14	1.1
Apatite	0.57	0.73	0.62	0.92	0.73	1.11	1.11	0.95	1.09	1.04	1.18	1.11
Total	98.21	98.66	97.92	99.94	97.3	97.64	98.22	96.44	97.51	97.72	97.08	97.47
D.I.	**84.91**	**89.39**	**88**	**89.61**	**84.96**	**81.4**	**83.24**	**77.16**	**82.13**	**82.54**	**80.19**	**82.03**

Tab. 7. Normative mineral compositions for the volcanic-sub-volcanic complex of G. El-Hajid

	Alkali granite									Porph. Granite		Rhyolite		
	100	**200**	**300**	**48**	**500**	**600**	**700**	**800**	**900A**	**30A**	**31**	**V10**	**V30**	400
Quartz	34.56	36.39	36.33	34.81	33.65	30.53	33.32	34.31	34.16	25.69	25.41	33.8	35.28	34.12
Corundum	0	0.8	2.08	0.09	0.68	0	0	1.29	0.15	0	0	0	0	0
Orthoclase	27.84	29.49	29.08	30.2	29.61	30.5	31.09	29.38	28.73	30.2	29.08	35.94	36.11	38.36
Albite	27.33	25.89	27.16	27.33	26.31	31.56	27.09	27.16	30.12	31.22	34.27	22.32	19.94	20.98
Anorthite	1.99	1.89	0.88	2.93	2.44	0	0	1.84	1.9	6.58	4.38	0	0	0.78
Acmite	0	0	0	0	0	2.09	3.19	0	0	0	0	2.77	4.57	0
Diopside	1.99	0	0	0	0	1.58	0.63	0	0	0.17	2.17	1.32	1.12	1.55
Hypersthene	0.96	2.04	1.9	1.45	1.95	1.42	2.08	2.16	1.62	1.73	0.67	1.18	1.51	0.12
Magnetite	1.7	1.65	1.62	1.33	1.83	0.82	0.11	2	1.51	2.64	2.45	1.25	0.09	2.29
Ilmenite	0.36	0.27	0.32	0.27	0.68	0.4	0.51	0.55	0.36	0.72	0.93	0.4	0.38	0.44
Apatite	0.09	0.07	0.02	0.07	0.14	0.05	0.12	0.07	0.05	0.09	0.26	0.02	0.02	0.07
Total	96.82	98.49	99.4	98.49	97.29	98.95	98.14	98.75	98.59	99.04	99.62	99	99.03	98.7
D.I.	**89.73**	**91.77**	**92.57**	**92.34**	**89.57**	**92.59**	**91.5**	**90.85**	**93.01**	**87.11**	**88.76**	**92.06**	**91.33**	**93.46**

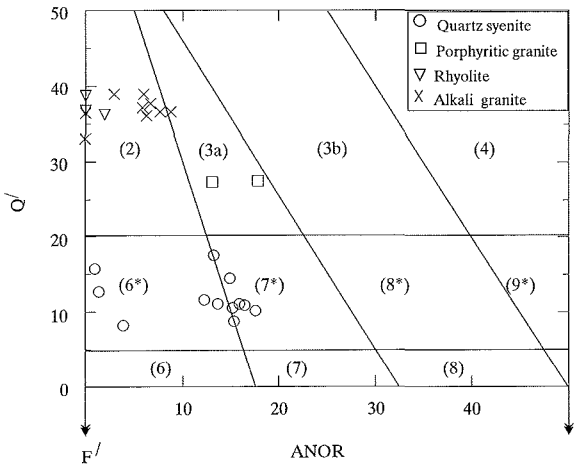

Fig. 3. Q/(F/)-ANOR diagram for normative classification of the rocks studied (after STRECKEISEN & LE MAITRE 1979); The symbols used are: O = quartz syenite, x = alkali granite, □ = porphyritic granite, ▽ = rhyolite

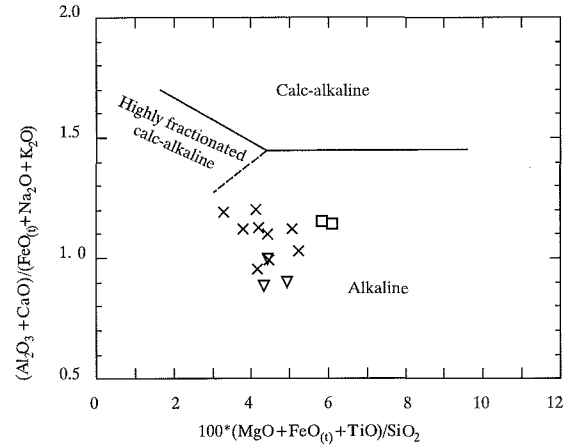

Fig. 4. $(Al_2O_3+CaO)/(FeO_{(t)}+Na_2O+K_2O)$ versus $100(MgO+FeO_{(t)}+TiO_2)/SiO_2$ diagram (SYLVESTER 1989)

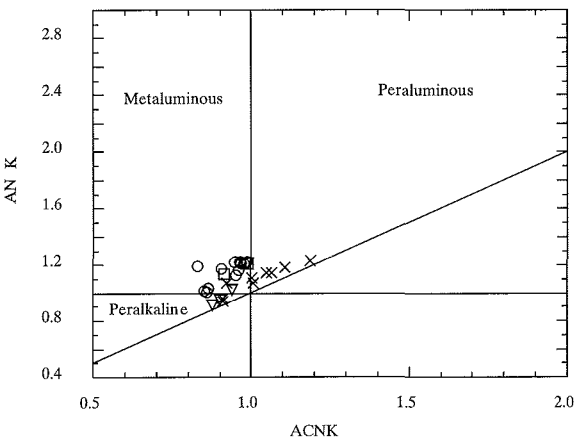

Fig. 5. $Al_2O_3/(Na_2O+K_2O)$ vs. $Al_2O_3/(CaO+Na_2O+K_2O)$ diagram (MANAIR & PICCOLI 1989)

The rocks of El-Hajid are chemically similar and are rich in Rb, Nb, Zr, and Y relative to the quartz syenite. K_2O/Na_2O ratios of the quartz syenite range from 1.31 to 1.57 with an average of 1.42. The alkali granite and the porphyritic granite of G. El-Hajid have nearly comparable values of K_2O/Na_2O (see Table 5), whereas the rhyolite contains the highest K_2O/Na_2O ratios (2.02 to 2.62). The K-enrichment in the rhyolite of G. El-Hajid will be discuss in detail in the petrogenesis section.

On the Q/(F/)-ANOR diagram (Text-fig. 3; STRECKEISEN & LE MAITRE 1979), the quartz syenite of G. Goza–G. Banat plots in the syenite fields (6* and 7*), while the volcanic-subvolcanic rocks of G. El-Hajid plot in the alkali rhyolite/granite fields (2 and 3a). The alkaline affinity of the silica-rich rocks is confirmed on the diagram of SYLVESTER (1989), which discriminates between alkaline, calc-alkaline and highly fractionated calc-alkaline granites with SiO_2 > 68 wt.% (Text-fig. 4). In terms of molar A/CNK $[Al_2O_3/(CaO+Na_2O+K_2O)]$ and the A/NK $[Al_2O_3/(Na_2O+K_2O)]$, the quartz syenite is metaluminous whereas data for the volcanic-subvolcanic complex plot in the metaluminous, peraluminous and peralkaline fields (Text-fig. 5). The peraluminous samples are characterized by normative corundum (0.09–2.58%), whereas the peralkaline samples contain normative acmite (2.09–4.57%).

On Harker diagrams (Text-figs 6, 7), the two felsic suites show one (more or less) consistent trend, especially in the trace elements which are less sensitive to secondary processes, with a compositional gap between 66.4 and 70.6 wt. % SiO_2. In each suite, Al_2O_3, Fe_2O_3, TiO_2, MgO, CaO, and P_2O_5 concentrations decrease with increasing SiO_2 content, whereas the contents of K_2O and Na_2O vary widely within the two suites. Regarding the trace elements, Nb, Y and Rb increase whereas Sr and Ba decrease with increasing SiO_2 content in each suite. Zr concentrations increase in the quartz syenite with increasing SiO_2 content, but its content varies widely in the more felsic suite of G. El-Hajid.

The overall geochemical characteristics of the studied rocks are consistent with a within-plate tectonic setting. All analyzed samples of the VSC of G. El-Hajid fall in the within-plate field on the Nb vs. Y diagrams of PEARCE & *al.* (1984), while the quartz syenite of G. Goza–G. Banat straddles the boundary between the within-plate and volcanic-arc fields (Text-fig. 8); however, both suites fall in

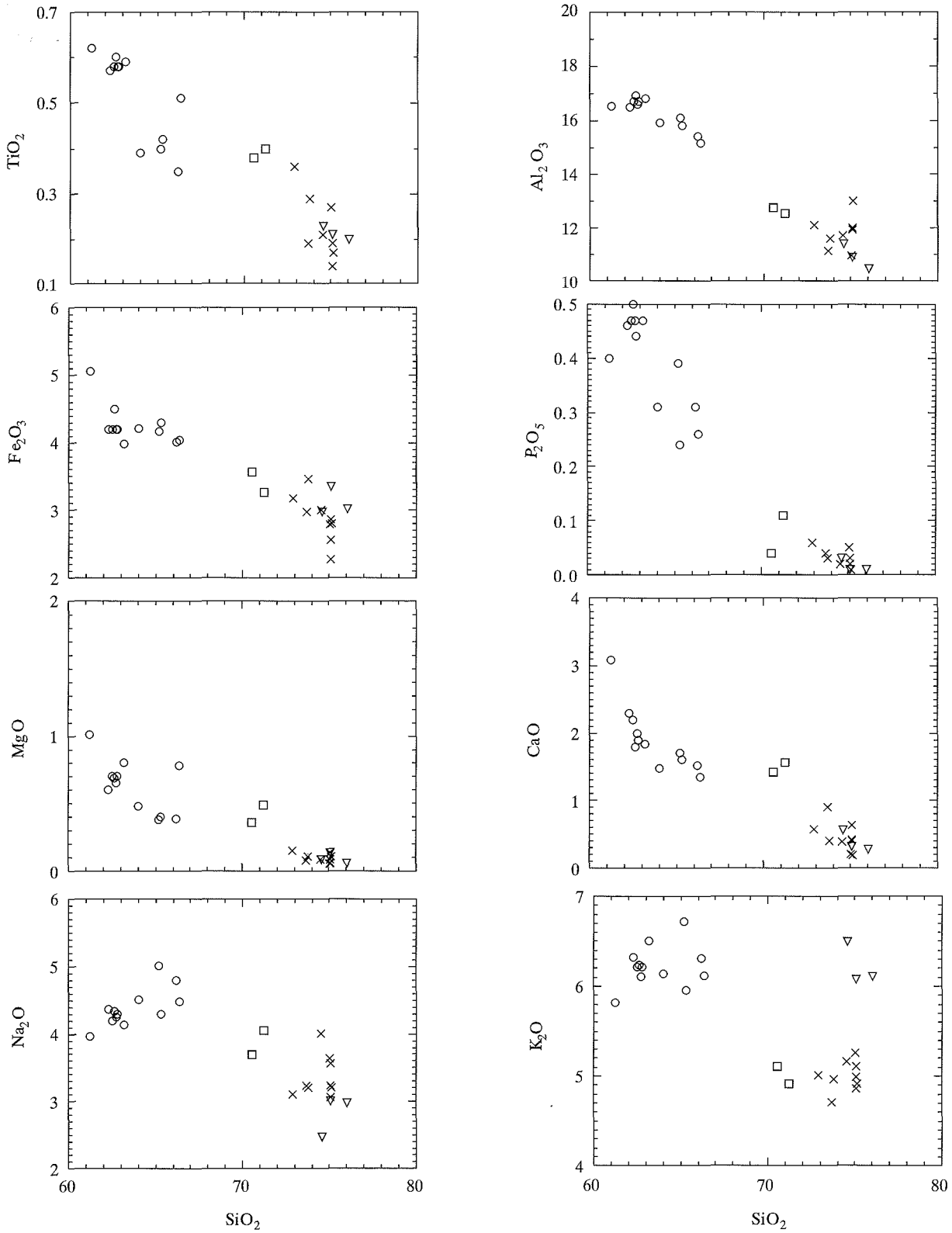

Fig. 6. The relation between SiO_2 and major oxides in the felsic alkaline suites

the field of A-type granites as delineated by STERN & GOTTFRIED (1989).

The concentrations of the REE in the representative samples are presented in Table 8. The distribution of the REE in the two felsic suites is characteristic of A-type granites, which are characterized by high contents in HFSE and REE (WHALEN & *al.* 1987). REE profiles of representative samples of the two suites are showing in Text-fig. 9. The REE profiles of the VSC of G. El-Hajid are quite similar with enrichment in the light REE [(La/Yb)n = 3.04-6.97], relatively flat heavy REE profiles [(Gd/Yb =1.18-1.32] and a strongly negative Eu-anomaly (Eu/Eu* = 0.12-0.29). The alkali granite contains the highest LREE, which is attributed to the presence of allanite. The REE profiles of the quartz syenite of G. Goza–G. Banat are also similar in that LREE are more enriched than HREE [(La/Yb)n= 5.33-5.70]. It shows either a slightly negative or positive Eu-anomaly (Eu/Eu*= 0.79-1.34).

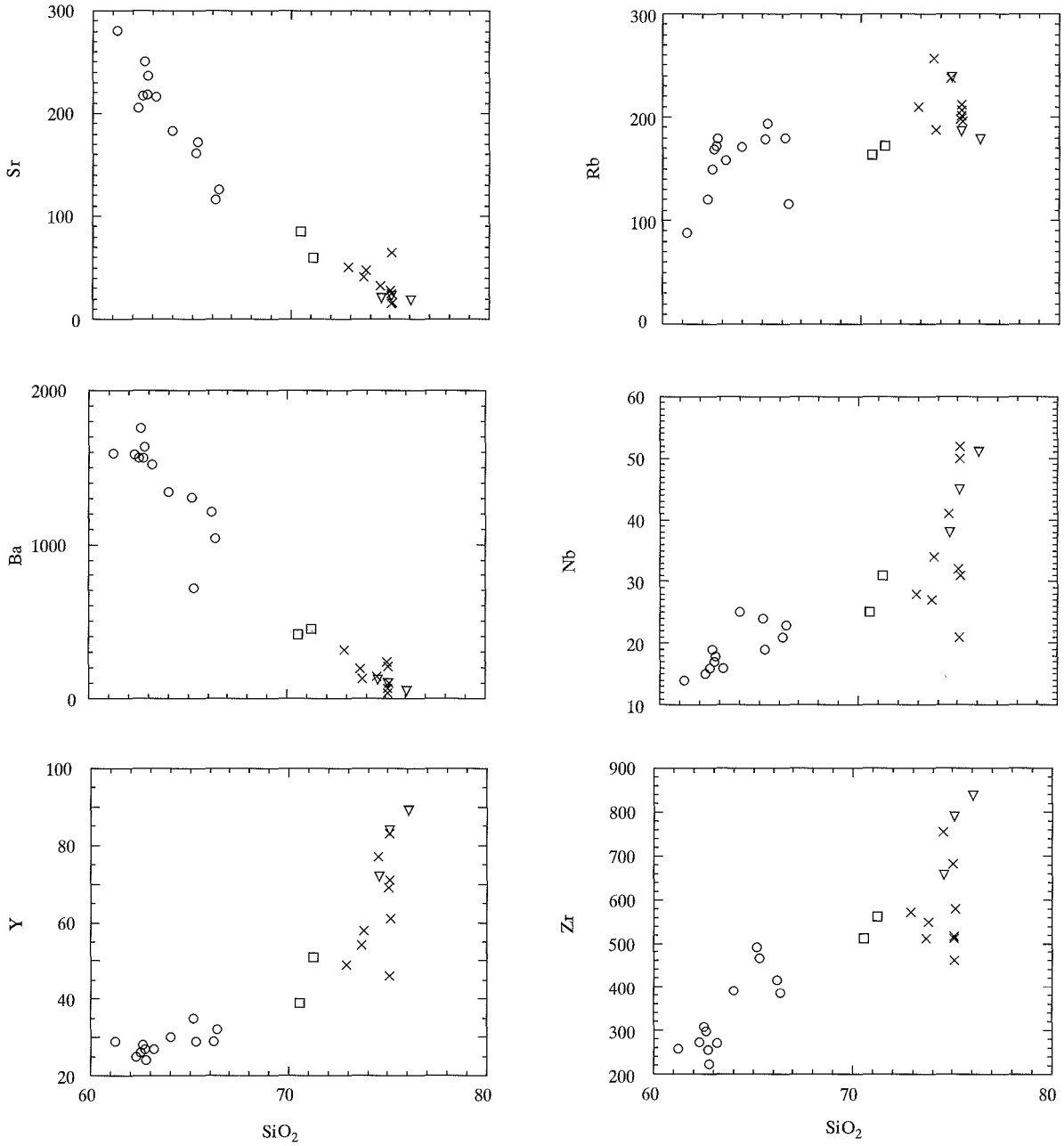

Fig. 7. The relation between SiO_2 and some trace elements in the felsic alkaline suites

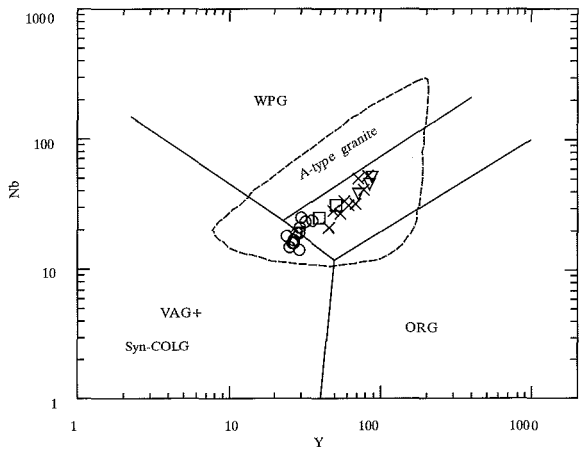

Fig. 8. Nb vs. Y diagram for the felsic alkaline suites (PEARCE & *al.* 1984); The dashed field represent A-type granites of WHALEN & *al.* (1987) delineated by STERN & GOTTFRIED (1989)

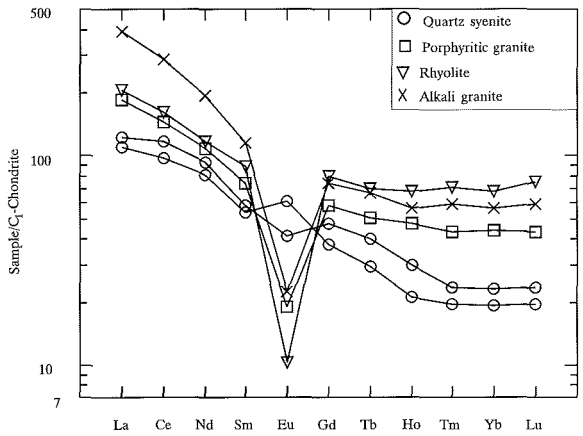

Fig. 9. Chondrite-normalized REE profiles for the felsic alkaline suites (using the chondrite values of EVENSEN & *al.* 1978)

The primitive mantle normalized multi-element diagram for the averages of the different rock types in the two suites is shown in Text-fig. 10. The more enhanced negative anomalies for Ba, Sr, Eu, and Ti are clear in the more evolved suite (G. El-Hajid) and probably reflects greater degrees of fractional crystallization.

CONDITIONS OF MAGMA CRYSTALLIZATION

The hypersolvus nature of the alkaline felsic suites suggests low water pressure (or low water content) and a high temperature of crystallization similar to that of other alkaline rocks emplaced at relatively shallow depth (TUTTLE & BOWEN 1958; MARTIN & BONIN 1976; LOWENSTERN & *al.* 1997). Moreover, all the rocks studied display the general characteristics of A-type and within-plate granites, which are characterized by high temperatures of crystallization ~900°C (COLLINS & *al.* 1982; CLEMENS & *al.* 1986; KING & *al.* 1997; KLIMM & *al.* 2003). The relatively shallow crustal levels of their emplacement is indicated by: (1) discordant lithologic contacts, (2) miarolitic cavities, (3) coeval volcanic and plutonic rocks of similar compositions, (4) relatively small crystal size of the plutonic rocks (up to 3 mm), and (5) the predominance of granophyric texture.

Sample	Quartz syenite		Volcanic-subvolcanic complex		
			Alkali granite	Porph. Granite	Rhyolite
	G20	B15	300	31	V30
La	27	30	96	45	50
Ce	62	75	184	93	103
Nd	38.1	43.8	91.2	51	55
Sm	8.3	8.9	17.6	11.42	13.6
Eu	3.5	2.4	1.3	1.1	0.6
Gd	7.7	9.7	15.2	11.85	16.2
Tb	1.1	1.5	2.5	1.9	2.6
Ho	1.2	1.7	3.2	2.7	3.8
Tm	0.5	0.6	1.5	1.1	1.8
Yb	3.2	3.8	9.3	7.3	11.1
Lu	0.5	0.6	1.5	1.1	1.9
ΣREE	153.1	178	423.3	227.47	259.6
(Eu/Eu*)n	1.34	0.79	0.24	0.29	0.12
(La/Yb)n	5.70	5.33	6.97	4.16	3.04
(Gd/Yb)n	1.94	2.06	1.32	1.31	1.18
(La/Sm)n	2.05	2.12	3.43	2.48	2.31
(Gd/Lu)n	1.91	2.01	1.26	1.34	1.06
(La/Lu)n	5.61	5.19	6.64	4.25	2.73

Tab. 8. REE analyses of representative samples

The presence of modal quartz in the quartz syenite indicates that the melt was above the Ab-Qz silica buffer (a_{SiO_2} =1) suggesting that the magma began to crystallize at 800–900°C (MITCHELL & PLATT 1978). CLEMENS & *al.* (1986) concluded that the minimum melt temperature of A-type granite magmas is 830°C (at 1 kbar) and may exceed 900°C. The relatively high temperature coupled with the fluxing effect of the halogens (especially fluorine) promotes fluidity which enables the magma to rise to high levels in the crust and to fill fractures. Garnet in the rhyolite of VSC at G. El-Hajid containing MnO>4 wt.% indicates crystallization from a silicic melt at shallow depths (≤ 5 kbar; GREEN 1977).

PETROGENESIS

Several petrogenetic models have been proposed for the genesis of A-type granites, including fractionation from mantle-derived basaltic magmas, interaction between mantle-derived magmas and crustal rocks, and anatexis of crustal rocks. Detailed reviews of these models were presented by COLLINS & *al.* (1982), CLEMENS & *al.* (1986), WHALEN & *al.* (1987), EBY (1990), and LANDENBERGER & COLLINS (1996). Despite the presence of different petrogenetic models for the generation of A-type granites, there is a general consensus that A-type granites were emplaced in both post-orogenic and anorogenic tectonic settings (WHALEN & *al.* 1987; SYLVESTER 1989; ROGERS & GREENBERG 1990; EBY 1990, 1992; PITCHER 1997; WU & *al.* 2002; LEE & *al.* 2003; MUSHKIN & *al.* 2003; TOLLO & *al.* 2004).

A-type granites in south Sinai belong to the latest stage of magmatic activity in the Arabian-Nubian Shield (BENTOR 1985; BENTOR & EYAL 1987), which marks the transition to intraplate alkaline magmatism. The origin of these granites is still a matter of debate because of the difficulty in assessing their tectonic environment and their protoliths. Plotting the analytical data on the Rb/Nb vs. Y/Nb diagram of EBY (1992) (Text-fig. 11) suggests that the felsic magmas of both suites were generated mainly by partial melting of crustal rocks. This assumption is substantiated by the predominance of evolved acid A-type rocks accompanied less commonly by syenitic rocks, and by the absence of more basic rocks. Experimental evidences reported by PATINO DOUCE (1997) indicated that dehydration melting of calc-alkaline tonalite at 950°C and 4 kbars, can produce melts with major and trace elements characteristics of A-type magmas. The enclosing older gneisses and the early phases of the calc-alkaline granitoids could probably therefore have produced the felsic suites studied.

The models proposed for the generation of syenitic rocks include: (1) partial melting of crustal rocks (LUBALA & *al.* 1994), (2) mantle origin (SUTCLIFFE & *al.* 1990; YANG & *al.* 2005), and (3) mixing of basic and silicic magmas with subsequent differentiation of the hybrid liquids (ZHAO & *al.* 1995; MINGRAM & *al.* 2000; RIISHUUS & *al.* 2005). The present study indicates that the quartz syenite of G. Goza–G. Banat represents the precursor, or the less evolved phase, of the A-type magmas in south Sinai. Direct derivation of this magma from a mantle source is difficult to reconcile with the available geochemical data which favour a crustal origin for the quartz syenite. Derivation of the quartz syenite from pure crustal melts is equally unlikely because such melts cannot be produced directly by anatexis (MONTEL & VIELZEUL 1997). Therefore, the most suitable mechanism for deriving the quartz syenite magma is by a process of hybridization, either by assimilation of crustal material by mantle-derived basaltic magmas or by mixing of the latter with crustal melts with subsequent differentiation of the hybrid liquids. This mechanism is supported by the presence of large mafic xenocrysts overgrown by primary K-feldspars.

The overall trends of major and trace elements (Text-figs 6, 7), the elemental ratios (Text-fig. 11) and the fractionated nature of the REE (Text-fig. 9) as well as the primitive mantle normalized multi-element diagram (Text-fig. 10) suggest that the two felsic suites are derived from the same magma, but were separated by a considerable time gap (period of magmatic quiescence). During this period of magmatic quiescence, the magma had undergone a high degree of fractional crystallization and/or crustal contamination which led to a composition gap between the two suites. Alkali feldspars were the main fractionating phase; fractionation of biotite, apatite and Fe-Ti oxides played a minor role. Fractionation of alkali feldspar is supported by plots of Rb and Ba against Sr (Text-fig. 12A, B), which suggest that alkali feldspar was the main fractionating phase (the trends of crystallization are adopted from MINGRAM & *al.* 2000). The two

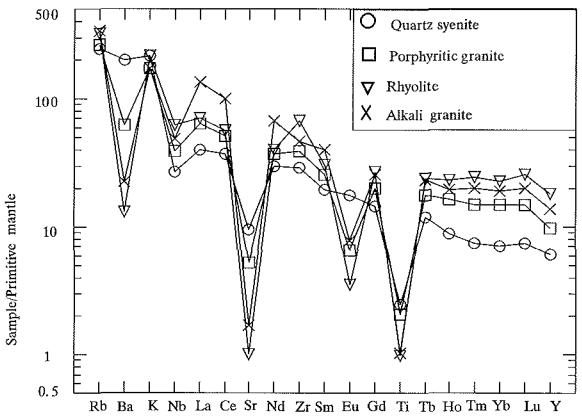

Fig. 10. Primitive mantle-normalized spider diagram for the felsic alkaline suites. Normalization values are taken from MCDONOUGH & *al.* (1991)

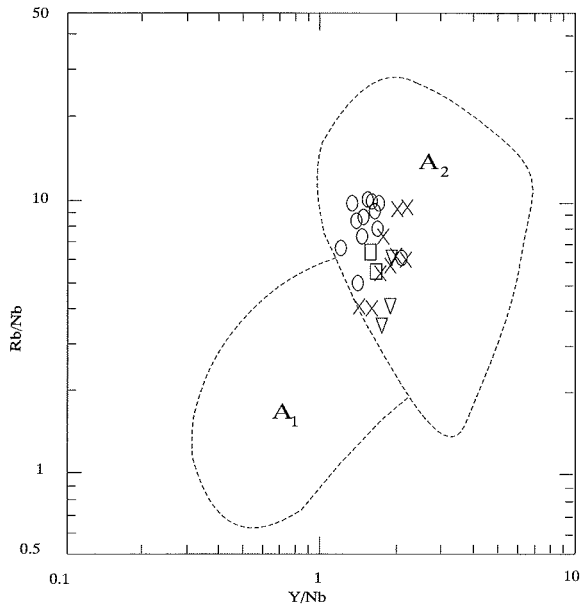

Fig. 11. Rb/Nb vs. Y/Nb diagram for distinction of A-type granitoids (EBY 1992). A_1=A-type granitoids with an OIB-type source, A_2= A-type granitoids with crustal derived magma

suites, especially the quartz syenite of G. Goza–G. Banat, show a wide range of K/Rb and Rb/Zr ratios (see Tables 4, 5), which can be taken as evidence that crustal contamination has played a role in their evolution. These ratios do not change significantly during fractional crystallization but change through crustal contamination (DAVIDSON & *al.* 1987, 1988). The role of crustal contamination in the evolution of quartz syenite of G. Goza–G. Banat is additionally confirmed by the presence of mafic xenocrysts.

In the present study, the high K_2O/Na_2O ratio is restricted to the rhyolite of G. El-Hajid. High K_2O/Na_2O ratios were observed in similar rocks in adjacent areas, for example, in the Neshef Massif, southern Israel, where AGRON & BENTOR (1981) suggested post-emplacement metasomatic replacement of Na by K. In south Sinai, AZER (2004) and SAMUEL & *al.* (2005) suggested a magmatic origin for the marked increase in potash content with marked decrease in soda and no indication of metasomatic substitution in similar rocks at G. El-Homra and Wadi El-Mahash.

The rocks of G. El-Hajid, both normal and K-rich, possess almost constant total alkali contents. In the K-rich rhyolite, potash appears to increase at the expense of soda. Many authors favour low or high temperature K-metasomatism for K-enrichment. Low-temperature K-metasomatism, involving a replacement of soda by potash by groundwater during alteration, is not feasible since the rhyolite is always fresh, no adulara has been detected and shows normal values of L.O.I. (0.58–0.93 %). High-temperature K-metasomatism assumes that potash-rich alkali rhyolites were derived from a normal alkali granitic magma that underwent alteration during or after emplacement (TAYLOR & *al.* 1984). Chemically, high-temperature K-metasomatism is characterized by an increase in K_2O, Rb, Zn and a decrease in Na_2O accompanied by depletion in the REE (KINNAIRD & *al.* 1985). The K-rich rhyolite and normal rocks studied have comparable contents of Zn and REE. Rubidium content in the K-rich rhyolite ranges from 179 to 239 ppm, which is not abnormally higher than in the other rock types in the area (see Table 5); a very high Rb content (≥1000 ppm) was reported in K-metasomatized rhyolitic rocks (KINNAIRD & *al.* 1985). The present data thus indicate that K-metasomatism is not a feasible mechanism for the explanation of the observed K-enrichment. This latter feature can

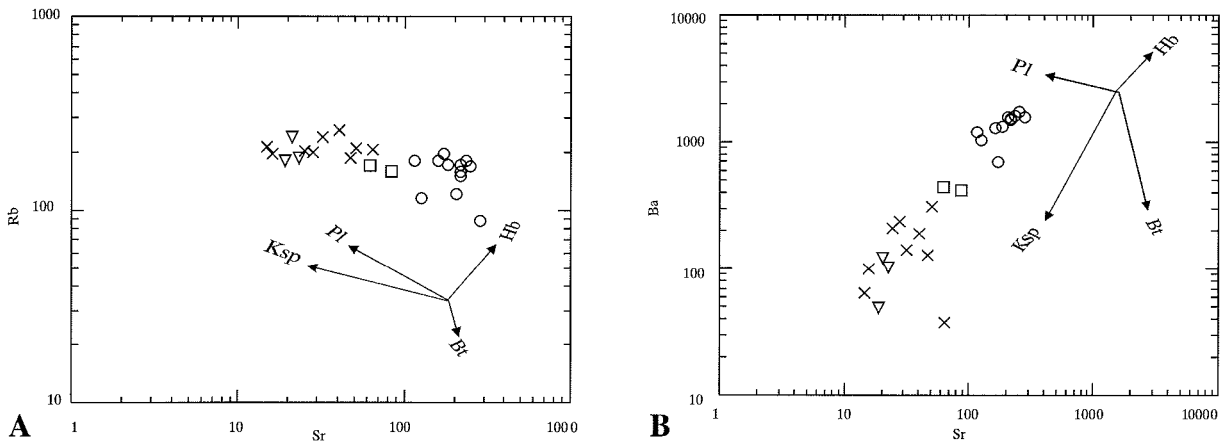

Fig. 12 (A-B). Some trace element relationships in the felsic alkaline suites. Hb: hornblende; Pl: plagioclase; Bt: biotite; Ksp: K-feldspar

therefore be attributed to the role of gas transfer at the late stage of magma crystallization (SAHAMA 1974).

The feasible mechanism suggested for the genesis of the K-rich rhyolite depends on the fact that Na_2O dissolves more readily than K_2O in the vapour phase accumulating in the upper part of the magma chamber. Given ample time for the volatiles dissolved in the magma to act and accumulate, the greater part of the Na_2O (and a smaller part of the K_2O) is lost to the accumulating, and later exploding gases. However, alumina remaining in the magma which cannot combine to form albite (due to loss of soda) or muscovite (due to deficiency in H_2O) would import more potash from the deeper levels of the magma chamber to form more K-feldspars. This explains adequately the increased potash content (seemingly at the expense of lost soda).

The possible heat source required for melting crustal rocks to generate A-type magmas is a matter of controversy. Experimental phase relations indicate that alkaline granites are formed at higher temperatures than their calc-alkaline counterparts and thus did not fractionate from them (CLEMENS & *al.* 1986). In south Sinai, lithospheric extension is expressed by strike-slip faults and emplacement of regional dyke swarms prior to emplacement of the alkaline rocks. These deep-seated faults, most probably represent reactivated Pan-African fractures formed during cooling, relaxation, and uplifting of the newly formed Pan-African crust (ABDEL-RAHMAN & EL-KIBBI 2001). These megafractures may cause pressure release at depth and influx of volatiles into the crust from the upper mantle. Such heated volatiles could initiate partial melting in the continental crust (BAILEY 1974). Pressure release by extension of fractures and increasing mantle contribution of hot volatiles are sufficient to cause partial melting of lower continental crustal rocks (HARRIS 1982).

A-TYPE ROCKS IN SOUTH SINAI

In south Sinai, A-type rocks comprising the Katherina Volcanics, alkaline granites, and a few ring complexes and dykes having an anorogenic signature erupted mostly during the time interval from 580 to 550 Ma (BIELSKI 1982). They occur as relatively small, scattered plutons or as dyke-like intrusions that encompass a wide range of compositions including sub-alkaline, transitional and alkaline/peralkaline granitoids (quartz syenite, syenite, quartz monzonite, monzonite, and alkaline/peralkaline granites) and their volcanic equivalents. A group of evolved granitic rocks commonly known as the Iqna granites, occur in south Sinai. They show mineralogical and geochemical characteristics common to A-type granites. They are late- to post-orogenic and were emplaced from 580 to 560 Ma ago (BIELSKI 1982). The Iqna granites of G. Katherina and W. Kid yielded Rb/Sr ages of 560±10 and 580±23 Ma respectively (BIELSKI 1982). The Iqna granites agree therefore, in their chemical compositions and age with the A-type granites in south Sinai. These granites are equivalent to A_2 granite subgroup of EBY (1992) and thus may belong to the highly fractionated calc-alkaline granite series (AZER 2006). The presence of such an overlap encourages the present author to separate the felsic rocks with A-type characteristics in south Sinai into several subgroups.

Based on the present work, as well as published data (EL-METWALLY 1997; EL-BAROUDY 1999; EL-TOKHI 2001; EL-SAYED 2001, 2003; AZER 2004, 2006; SAMUEL & *al.* 2005 and others), the present author distinguished the felsic igneous rocks with A-type characteristics in south Sinai according to magma source and tectonic setting into (1) non-primitive A-type magma (A_{NP}) and (2) primitive A-type magma (A_P). The non-primitive A-type magma includes the Iqna granites in south Sinai which include the highly fractionated, late- to post-orogenic, calc-alkaline I-type granites. The primitive A-type magma is a typical within-plate anorogenic magma. It is distinguished further into: (i) A-type magma having an OIB-mantle character (A_1) and (ii) A-type magma of crustal source (A_2). The A_1 and A_2 categories originate from EBY (1992). The general characteristics of the non-primitive and primitive A-type magmas, based on the present study and compilation of data from whole Sinai, are summarized in Table 9. Further investigation involving the determination of isotopic ratios will be done to justify the proposed origin of the alkaline felsic suites in south Sinai.

CONCLUSIONS

The studied felsic suites occur as dyke-like intrusions cross cutting late Pan-African, subduc-

	Non-primitive A-type magma (A_{NP})	Primitive A-type magma (A_P)	
		A_1	A_2
Age	580-560 Ma	580-550 Ma	
Field	Form circular to oval high mounts with sharp contacts; contain rare enclaves and cut by few dykes	Circular to oval shape or dyke-like intrusions and ring complexes; devoid of enclaves and dykes	
Rock types	Alkali feldspar granite, syenogranite and less common monzogranite	Alkaline to peralkaline granite, quartz syenite and syenite as well as their volcanic equivalents	Alkali feldspar granite, quartz syenite and their volcanic equivalents
Mafic minerals	Mainly biotite± hornblende (<5% wt. %)	Alkali amphibole and rare biotite (1-12 %)	Biotite± calcic or sodic-calcic amphibole (<2 %)
Tectonic setting	Late to post-orogenic	Anorogenic	
Magma type	Calc-alkaline with some alkaline tendency	Alkaline to peralkaline	
	Equivalent to A_2 of EBY (1992)	Equivalent to A_1 of EBY (1992)	Equivalent to A_2 of EBY (1992)
Genesis	Highly fractionated calc-alkaline I-type magma	A-type magma derived from mantle-crustal source	A-type magma derived mainly from partial melting of crustal rocks
Differentiation process	Strong fractional crystallization and magma mixing	Extreme fractional crystallization and subsolidus interactions	
Examples	Iqna granite (W. Iqna; W. Kid)	Katherina Volcanics at G. El-Homra; alkaline granite at G. Musa; quartz syenite of Katherina ring complex	The volcanic rocks of W. El-Mahash and W. Khileifiya; quartz syenite of G.Goza-G. Banat; volcanic-subvolcanic complex G. El-Hajid

Tab. 9. Classification of A-type magmas at South Sinai

tion-related calc-alkaline batholiths and highly fractionated calc-alkaline granites (Iqna granite). Emplacement of these intrusions was preceded by intrusion of dyke swarms of variable compositions that were formed during an extensional regime and which mark the transition from calc-alkaline to alkaline magmatism (FRIZ-TÖPFER 1991). Emplacement of the alkaline felsic intrusions was therefore controlled by pre-existing fractures developed in an extensional tectonic regime at the end of the Pan-African orogeny.

The two felsic suites possess all the main features of A-type granites which are formed during an anorogenic stage and were emplaced as relatively hot (~900°C) magma at shallow depth (≤5 kbar). They are cogenetic and might have been formed by fractionation of melts derived from a continental source with mantle contribution (especially in the case of the quartz syenite). The two suites were separated by a considerable time gap which led to a formation of composition gap between them. The K-enrichment in the rhyolite of G. El-Hajid is attributed to the effect of volatiles accumulated in the upper part of the magma chamber together with the fact that Na_2O dissolves more readily than K_2O in the vapour phase.

The quartz syenite of G. Goza–G. Banat represents the least evolved phase of the A-type granites in south Sinai. Geochemically, the quartz syenite of G. Goza–G. Banat is distinguished from the quartz syenite of the Katherina area in southern Sinai (EL-TOKHI 2001). The former has the geochemical characteristics of A_2 subgroup of EBY (1992), while the latter shows the characteristics of A_1 subgroup (op. cit) which indicates that quartz syenites in southern Sinai have different sources. The volcanic-subvolcanic complex (VSC) of G. El-Hajid represent the more evolved phase of A-type granites in south Sinai. It may represents part of the Katherina ring complex, including alkaline lavas which erupted during cauldron subsidence. The magma that ponded beneath the caldera structure was emplaced as composite resurgent intrusions of volcanic and subvolcanic rocks that are highly variable in texture. A-type magmas in south Sinai are distinguished according to their magma source and tectonic setting into (1) non-primitive A-type magma (A_{NP}) and (2) primitive A-type magma (A_P).

Acknowledgement

The author is greatly indebted to Prof. EL-GABY for his fruitful discussions and critical reading for the manuscript. Also, he would like to express deep gratitude to geologist Ghazi Abdul HAY for performing the chemical analyses at the Saudi Arabia Geological Survey.

REFERENCES

ABDEL-RAHMAN, A.M. & EL-KIBBI, M.M. 2001. Anorogenic magmatism: chemical evolution of the Mount El-Sibai A-type complex (Egypt), and implications for the origin of within-plate felsic magmas. *Geological Magazine*, **138**, 67-85.

AGRON, N. & BENTOR, Y.K. 1981. The volcanic massif of Biq'at Hayareah (Sinai-Negev): A case of potassium metasomatism. *Journal of Petrology*, **89**, 479-495.

AZER, M.K. 2004. Petrological and geochemical studies of some volcanic rocks at South Sinai, Egypt. Ph. D. Thesis, Faculty of Science, Cairo Univ., 130 pp.

— 2006. Tectonic significance of Late Precambrian calc-alkaline and alkaline magmatism in South Sinai, Egypt. (Accepted to *Geologica Acta*).

BAILEY, D.K. 1974. Origin of alkaline magmas as a result of anatexis, (b) crustal anatexis. *In*: SORENSON, H. (*Ed.*), The alkaline rocks, pp. 436-442. *Wiley & Sons*; London.

BENTOR, Y.K. 1985. The crustal evolution of the Arabo-Nubian Massif with special reference to Sinai Peninsula. *Precambrian Research*, **28**, 1-74.

BENTOR, Y.K. & EYAL, M. 1987. The geology of Sinai, its implication for the evolution of the Arabo-Nubian Massif, Jebel Sabbagh sheet. The Israel Academy of Sciences and Humanities, 484 pp.

BIELSKI, M. 1982. Stages in the evolution of the Arabian-Nubian Massif in Sinai. Ph.D. Thesis, Hebrew Univ., Gerusalam, 155 pp.

BLASBAND, B., WHITE, S.H., BROOIJMANS, P., VISSER, W. & DE BOORDER, H. 2000. Late Proterozoic collapse in the Arabian-Nubian Shield. *Journal of Geological Society of London*, **157**, 615-628.

CHEN, B. & JAHN, B.M. 2004. Genesis of post-collisional granitoids and basement nature of the Junggar Terrane, NW China: Nd-Sr isotope and trace element evidence. *Journal of Asian Earth Sciences*, **23**, 691-703.

CLEMENS, J.D., HOLLOWAY, G.R. & WHITTE, A.G.R. 1986. Origin of the A-type granite: experimental constraints. *American Mineralogist*, **71**, 317-324.

COLLINS, W.J., BEAMS, S.D., WHITE, A.J.R. & CHAPPELL, B.W. 1982. Nature and origin of A-type granites with particular reference to southeastern Australia. *Contribution to Mineralogy and Petrology*, **80**, 189-200.

DAVIDSON, J.P., FERGUSON, K.M., COLUCCI, M.T. & DUNGAN, M.A. 1987. The origin of magmas from the San-Pedro-Pellado Volcanic Complex, South Chile: multicomponent sources and open system evolution. *Contribution to Mineralogy and Petrology*, **100**, 429-445.

DAVIDSON, J.P., DUNGAN, M.A., FERGUSON, K.M. & COLUCCI, M.T. 1988. Crust-magma interactions and the evolution of arc magmas: the San Pedro-Pellado Volcanic Complex Southern Chilean Andes. *Geology*, **15**, 443-446.

DEER, W.A., HOWIE, R.A. & ZUSSMAN, J. 1992. An introduction to the rock forming minerals. Second Edition, Longman Scientific and Technical, London, 696 pp.

EBY, G.N. 1990. The A-type granitoids: A review of their occurrence and chemical characteristics and speculations on their petrogenesis. *Lithos*, **26**, 115-134.

— 1992. Chemical subdivision of the A-type granitoids: Petrogenetic and tectonic implications. *Geology*, **20**, 641-644.

EL-BAROUDY, A.F. 1999. Petrogenesis and evolution of the alkali granites northwest Sharm El-Sheikh, southern Sinai, Egypt. The Fourth International Conference on Geochemistry, Alexandria Univ., Egypt, 447-466.

EL-GABY, S. 1975. Petrochemistry and geochemistry of some granites from Egypt. *Neues Jahrbuch für Mineralogie*, **124**, 147-189.

EL-GABY, S. & AHMED, A.A. 1980. The Feiran-Solaf gneiss belt, SW Sinai, Egypt. *Bull. Inst. Applied Geology, King Abdul Aziz University, Jeddah*, **3** (4), 95-105.

EL-HINNAWI., M. (*Ed.*) 1994. Geological map of Sinai, sheet No. 1, scale 1: 250 000. Geological Survey of Egypt.

EL-METWALLY, A.A. 1997. Origin and emplacement of a reversely zoned, Pan-African granitoid pluton from Sinai Massif, Egypt. *Journal of African Earth Sciences*, **24**, 29-38.

EL-RAMLY, M.F. & AKAAD, M.K. 1960. The basement complex in the central Eastern Desert of Egypt between Lat. 24° 30′ and 25° 40′ N. Geological survey of Egypt, Paper No. 8.

EL-SAYED, A.A. 2001. The A-type granites of Wadi El-Malha El-Rayan southeastern Sinai, Egypt: petrogenesis and radioactivity. *Egyptian Journal of Geology*, **45**, 633-651.

EL-SAYED, M.M. 2003. Neoproterozoic magmatism in

NW Sinai, Egypt: magma source and evolution of collision-related intracrustal anatectic leucogranite. International *Journal of Earth Science*, **92**, 145-164.

EL-SHAFEI, M.K. & KUSKY, T.M. 2003. Structural and tectonic evolution of the Neoproterozoic Feiran-Solaf metamorphic belt, Sinai Peninsula: implications for the closure of the Mozambique Ocean. *Precambrian Research*, **123**, 269-293.

EL-SHESHTAWI, Y.A. 1984. Petrographical and geochemical studies of granitic rocks around Wadi El-Sheikh, southwestern Sinai, Egypt. Ph.D. Thesis, Al-Azhar Univ., Egypt.

EL-TOKHI, M, 1990. Petrographical, geochemical and experimental studies on the migmatite rocks of Wadi Feiran, Southern Sinai, Egypt. Ph.D. Thesis, Karlsruhe Univ., Germany.

— 2001. Petrogenesis and geochemistry of some quartz-syenites from Southern Sinai, Egypt. The second International Conference on the Geology of Africa, Assiut University, Egypt, 239-253.

EVENSEN, N.M., HAMILTON, P.J. & O'NIONS, R.K. 1978. Rare earth abundances in chondritic meteorites. *Geochimica et Cosmochimica Acta*, **42**, 1199-1212.

EYAL, M. & HEZKIYAHU, T. 1980. Katherina pluton: the outline of a petrologic framework. *Israel Journal of Earth Science*, **29**, 41-52.

FRIZ-TÖPFER, A. 1991. Geochemical characterization of Pan-African dyke swarms in southern Sinai: from continental margin to intraplate magmatism. *Precambrian Research*, **49**, 281-300.

GHARIB, M.E. & OBEID, M.A. 2004. Geochemistry and evolution of the Neoproterozoic granitoid magmatism in the Wadi El-Sheikh-Gabal Saint Katherina area, Southwestern Sinai, Egypt. 7th International Conference on the Geology of the Arab World, 53-73.

GREEN, T.H. 1977. Garnet in silicic liquids and its possible use as a P-T indicator. *Contributions to Mineralogy and Petrology*, **65**, 59-67.

HARRIS, N.B.W. 1982. The petrogenesis of alkaline intrusives from Arabia and Northeast Africa and their implications for within-plate magmatism. *Tectonophysics*, **83**, 243-258.

HUSSEIN, A.A., ALI, M.M. & EL RAMLY, M.F. 1982. A proposed new classification of the granites of Egypt. *Journal of Volcanology and Geothermal Research*, **14**, 187-198.

JAHN, B.M., WU, F.Y., CAPDEVILA, R., FOURCADE, S., WANG, Y.X. & ZHAO, Z.H. 2001. Highly evolved juvenile granites with tetrad REE patterns: the Woduhe and Baerhe granites from the Great Xing'an (Khingan) Mountains in NE China. *Lithos*, **59**, 171-198.

JAHN, B.M., CAPDEVILA, R., LIU, D.Y., VERNON, A. & BADARCH, G. 2004. Sources of Phanerozoic granitoids in the transect Bayanhongor-Ulaan Baatar, Mongolia: geochemical and Nd isotopic evidence, and implication for Phanerozoic crustal growth. *Journal of Asian Earth Sciences*, **23**, 629-653.

JOHNSON, P. 2003. Post-amalgamation basins of the NE Arabian Shield and implications for Neoproterozoic III tectonism in the Northern East African Orogen. *In*: KUSKY, T., ABDELSALAM, M., TUCKER, R. & STERN, R. (*Eds*), Evolution of the east African and Related Orogens. *Precambrian Research*, **123**, 321-337.

KATZIR, Y., EYAL, M., LITVINOVSKY, B.A., JAHN, B.M., ZANVILEVICH, A.N., VALLEY, J.W., BEERI, Y., PELLY, I. & SHIMSHILASHVILI, E. 2006. Petrogensis of A-type granites and origin of vertical zoning in the Katherina pluton, Gebel Mussa (Mt. Moses) area, Sinai, Egypt. *Lithos* (in press).

KING, P.L., WHITE, A.J.R., CHAPPEL, B.W. & ALLEN, C.M. 1997. Characterization and origin of aluminous A-type granites from the Lachlan Fold Belt, southeastern Australia. *Journal of Petrology*, **38**, 371-391.

KINNAIRD, J.A., BOWDEN, P., IXER, R.A. & ODLING, N.W.A. 1985. Mineralogy, geochemistry and mineralization of the Ririwai complex, northern Nigeria. *Journal of Africa Earth Science*, **3**, 185-222.

KLIMM, K. HOLTZ, F., JOHANNES, W. & KING, P.L. 2003. Fractionation of metaluminous A-type granites: an experimental study of the Wangrah Suite, Lachlan Fold Belt, Australia. *Precambrian Research*, **124**, 327-341.

KLITZSCH, E., LIST, F.K. & PÖHLMANN, G. (*Eds*), 1987. Geological map of Egypt, scale 1: 500 000, EGPC-CONOCO, Cairo, Egypt.

KRÖNER, A. 1985. Ophiolites and the evolution of tectonic boundaries in the late Proterozoic Arabian-Nubian Shield of northeast Africa and Arabia. *Precambrian Research*, **27**, 277-300.

KRÖNER, A., EYAL, M. & EYAL, Y. 1990. Early Pan-African evolution of the basement around Elat, Israel, and Sinai Peninsula revealed by single-zircon evaporation dating, and implication for crustal accretion rates. *Geology*, **18**, 545-548.

KRÖNER, A., GREILING, R., REISCHMANN, T., HUSSEIN, I.M., STERN, R.J., DURR, S., KRUGER, J. & ZIMMER, M. 1987. Pan-African crustal evolution in northeast Africa. *In*: KRÖNER, A. (*Ed.*), Proterozoic Lithospheric Evolution. *American Geophysical Union, Geodynamic Series*, **17**, 235-257.

KUSKY, T.M. & MATSAH, M. 2003. Neoproterozoic dextral faulting on the Najd fault system, Saudi Arabia, pre-

ceded sinistral faulting and escape tectonics related to closure of the Mozambique Ocean. *In*: YOSHIDA, M. & WINDLEY, B.F. (*Eds*), Proterozoic East Gondwana: Supercontinent Assembly and Breakup. *Geological Society of London, Special Publication*, **206**.

LANDENBERGER, B. & COLLINS, W.J. 1996. Derivation of A-type granites from a dehydrated charnockitic lower crust: evidence from the Chaelundi Complex, Eastern Australia. *Journal of Petrology*, **37**, 145-170.

LEE, S.R., CHO, M., CHEONG, C.S., KIM, H. & WINGATE, M.T.D. 2003. Age, geochemistry and tectonic significance of Neoproterozoic alkaline granitoids in the northwestern margin of the gyeonggi massif, South Korea. *Precambrian Research*, **122**, 297-310.

LOIZENBAUER, J., WALLBREEHER, E., FRITZ, H. NEUMAYR, P. KHUDEIR, A.A. & KLOETZLI, U. 2001. Structural geology, simple zircon ages and fluid inclusion studies of the Meatiq metamorphic core complex: Implications for Neoproterozoic tectonics in the Eastern Desert of Egypt. *Precambrian Research*, **110**, 357-383.

LOWENSTERN, J.R., CLYNNE, N.A. & BULLEN, T.D. 1997. Comagmatic A-type granophyre and rhyolites from the Alid Volcanic Center, Eritrea Northeast Africa. *Journal of Petrology*, **38**, 1707-1721.

LUBALA, R.T., FRICK, C., RODERS, J.H. & WALRAVEN, F. 1994. Petrogenesis of syenites and granites of the Schiel Alkaline complex. Northern Transvaal, South Africa. *Journal of Geology*, **102**, 307-309.

MANIAR, P.D. & PICCOLI, P.M. 1989. Tectonic discrimination of granitoids. *Geological Society of America Bulletin*, **101**, 635-643.

MARTIN, R.F. & BONIN, B. 1976. Water and magma genesis: the association hypersolvus granite-subsolvus granite. *Canadian Mineralogist*, **14**, 228-237.

MCDONOUGH, W.F., SUN, S., RINGWOOD, A.E., JAGOUTZ, E. & HOFMAN, A.W. 1991. K, Rb and Cs in the earth and moon and the evolution of the earth's mantle. *Geochimica Et Cosmochimica Acta*, Ross Taylor Symposium volume.

MINGRAM, B., TRUMBULL, R.B., LITTMAN, S. & GERSTENBERGER, H. 2000. A petrogenetic study of anorogenic felsic magmatism in the Cretaceous Paresis ring complex, Namibia: evidence for mixing of crust and mantle derived components. *Lithos*, **54**, 1-22.

MITCHELL, R.H. & PLATT, R.G. 1978. Mafic mineralogy of ferroaugite syenite from the Goldwell Complex, Ontariuo, Canada. *Journal of Petrology*, **19**, 627-651.

MONTEL, J.M. & VIELZEUF, D. 1997. Partial melting of greywackes: PartII. Composition of minerals and melts. *Contribution to Mineralogy and Petrology*, **128**, 176-196.

MUSHKIN, A., NAVON, O., HALICZ, L., HARTMANN, G. & STEIN, M. 2003. The petrogenesis of A-type magmas from the Amram Massif, southern Israel. *Journal of Petrology*, **44**, 815-832.

PATINO DOUCE, A.E. 1997. Generation of metaluminous A-type granites by low-pressure melting of calc-alkaline granitoids. *Geology*, **25**, 743-746.

PEARCE, J.A., HARRIS, N.B.W. & TINDLE, A.G. 1984. Trace element discrimination diagrams for the tectonic interpretation of granitic rocks. *Journal of Petrology*, **25**, 956-983.

PITCHER, W.S. 1997. The nature and origin of granite, 386 pp. *Chapman and Hall*; London.

RICHARD, L.R. 1995. Mineralogical and petrological data processing system. Minpet Software (C), 1988-1985, Version 2.02.

RIISHUUS, M.S., PEATE, D.W., TEGNER, C.T., WILSON, G.R., BROOKS, C.K. & WAIGHT, T.E. 2005. Petrogenesis of syenites at a rifted continental margin: origin, contamination and interaction of alkaline mafic and felsic magmas in the Astrophyllite Bay Complex, East Greenland. *Contribution to Mineralogy and Petrology*, **149**, 350-371.

ROGERS, J.J.W. & GREENBERG, J.K. 1990. Late-orogenic, post-orogenic and anorogenic granites: distinction by major-element and trace-element chemistry and possible origins. *Journal of Geology*, **98**, 291-309.

SAHAMA, Th. G. 1974. Potassium-rich alkaline rocks. *In*: SORENSEN, H. (*Ed.*), The alkaline rocks, pp. 96-109. *John Wiley and Sons*; New York.

SAMUEL, M.D., MOUSSA, H.E. & AZER, M.K. 2005. Alkaline volcanics from Taba-Nuweiba district, Central Eastern Sinai, Egypt. *Egyptian Journal of Geology*, **48**, 115-147.

STERN, R.J. 1994. Arc assembly and continental collision in the Neoproterozoic East African Orogen: implications for the consolidation of Gondwanaland. *Annual Review Earth Planetary Science*, **22**, 319-351.

STERN, R.J. & MANTON, W.I. 1987. Age of Feiran basement rocks, Sinai: implications for late Precambrian crustal evolution in the northern Arabian-Nubian Shield. *Journal of Geological Society of London*, **144**, 569-575.

STERN, R.J. & GOTTFRIED, D. 1989. Discussion of the paper "Late Pan-African magmatism and crustal development in northeastern Egypt". *Geological Journal*, **24**, 371-374.

STRECKEISEN, A. & LE MAITRE, R.W. 1979. A chemical approximation to the modal QAPF classification of

igneous rocks. *Neues Jahrbuch für Mineralogie Abhandlungen*, **136**, 169-206.

SUTCLIFFE, R.H., SMITH, A.R., DOHERTY, W. & BARNETT, R.L. 1990. Mantle derivation of Archean amphibole-bearing granitoids and associated mafic rocks: evidence from the southern Superior Province, Canada. *Contribution to Mineralogy and Petrology*, **105**, 255-274.

SYLVESTER, P.J. 1989. Post-collisional alkaline granites. *Journal of Geology*, **97**, 261-280.

TAYLOR, H.P., TURI, B. & CUNDARI, A. 1984. $^{18}O/^{16}O$ and chemical relationships in K-rich rocks from Australia, East Africa, Antarctica and San Venanzo-Cupaello, Italy. *Earth Planetary Science and Letters*, **69**, 263-276.

TOLLO, R.P., ALEINIKOFF, J.N., BARTHOLOMEW, M.J. & RANKIN D.W. 2004. Neoproterozoic A-type granitoids of the central and southern Appalachians: intraplate magmatism associated with episodic rifting of the Rodinian supercontinent. *Precambrian Research*, **128**, 3-38.

TUTTLE, C.F. & BOWEN, N.L. 1958. Origin of granite in the light of experimental studies in the system $NaAlSi_3O_8$-$KAlSi_3O_8$-SiO_2-H_2O. *Geological Society of America Memoir*, **74**, 153 pp.

WHALEN, J.B., CURRIE, K.L. & CHAPPELL, B.W. 1987. A-type granites: geochemical characteristics, discrimination and petrogenesis. *Contribution to Mineralogy and Petrology*, **95**, 407-419.

WU, F.Y., SUN, D.Y., LI, H., JAHN, B.M. & WILDE, S. 2002. A-type granites in northeastern China: age and geochemical constraints on their petrogenesis. *Chemical Geology*, **187**, 143-173.

WU, F.Y., SUN, D.Y., JAHN, B.M. & WILDE, S. 2004. A Jurassic garnet-bearing granitic pluton from NE China showing tetrad REE patterns. *Journal of Asian Earth Sciences*, **23**, 731-744.

YANG, J.H., CHUNG, S.L., WILDE, S.A., WU, F.Y., CHU, M.F., LO, C.H. & FAN, H.R. 2005. Petrogenesis of post-orogenic syenites in the Sulu Orogenic Belt, East China: geochronological, geochemical and Nd-Sr isotopic evidence. *Chemical Geology*, **214**, 99-125.

ZEN, E. 1988. Phase relations of peraluminous granitic rocks and their petrogenetic implications. *Annual Review of Earth and Planetary Sciences*, **16**, 21-51.

ZHAO, J.X., SHIRAISHI, K., ELLIS, D.J. & SHERATON, J.W. 1995. Geochemical and isotopic studies on syenites from the Yamoto Mountains, East Antartica: implication for the origin of syenitic magmas. *Geochimica et Cosmochimica Acta*, **59**, 1363-1385.

Manuscript submitted: 20th August 2006
Revision version accepted: 25th November 2006